Peer-reviewed version available at Sensors 2019, 19, 2305; doi:10.3390/s19102305

Article

Multi-stage Hough Space Calculation for Lane Mark Detection via IMU and Vision Data Fusion

Yi Sun, Jian Li* and ZhenPing Sun

National University of Defense Technology, Changsha 410073, China; 15575191281@163.com(YS)
* Correspondence:lijian@nudt.edu.cn; Tel.: +8613367319240

Abstract: It's challenging to achieve robust lane detection depending on single frame when considering complicated scenarios. In order to detect more credible lane markings by using sequential frames, a novel approach to fusing vision and Inertial Measurement Unit (IMU) is proposed in this paper. The hough space is employed as the space where lane markings are stored and it's calculated by three steps. Firstly, a basic hough space is extracted by Hough Transform and primary line segments are extracted from it. In order to measure the possibility about line segments belong to lane markings, a CNNs based classifier is introduced to transform the basic hough space into a probabilistic space by using the networks outputs. However, this probabilistic hough space based on single frame is easily disturbed. In the third step, a filtering process is employed to smooth the probabilistic hough space by using sequential information. Pose information provided by IMU is applied to align hough spaces extracted at different times to each other. The final hough space is used to eliminate line segments with low possibility and output those with high confidence as the result. Experiments demonstrate that the proposed approach has achieved a good performance.

Keywords: IMU; Vision; Classification Networks; Hough Transform;Lane Markings Detection

1. Introduction

As the development of artificial intelligence, intelligent driving technology has made great progress depend on different kinds of sensors and powerful computational capabilities of processors. It's a trend that intelligent vehicles play important roles in a safe and efficient transportation environment. Lane detection is an essential research field of intelligent driving, which could be employed to provide lane departure warning in Advanced Driver Assistance System (ADAS), and also could be used to give a local road navigation for autonomous vehicle especially when the GPS signal is disturbed.

A lot of methods are proposed to make lane detection system more robust. Line segments extraction is usually a common step to detect lane markings. Well-known methods like Hough Transform and LSD are employed in many works. However, there would exist a few false line segments in the result of line segments extraction such as those on cars or rails, post-process is necessary to distinguish whether these line segments are belong to lane markings or not. Geometry constraints like width-based constraints are always used in this kind of classification but it's hard to deal with some line segments such as those on rails when they satisfy most of geometry constraints. Meanwhile, appearance feature is good for object classification and CNNs based classifier have achieved good performance on many public datasets. Lots of end-to-end networks are proposed to detect lanes in image, but it's difficult to merging human's logistical knowledge into the networks and large amounts of labeled images are necessary.

Due to the disturbance of different kinds of noise, detection results extracted from single frame are not reliable for system control. It is important for achieving robust lane markings detection by integrating sequential information. Lane curvature tracking or the tracking of lane markings position are employed frequently in many works. However, the movement information of vehicle, which is the key factor in the tracking of lane markings, is usually obtained by estimation. The estimation error

would become obvious at large time scale and make it hard to track lane markings from a more global perspective.

In order to solve problems mentioned above, a novel approach is proposed to extract lane markings by the fusion of vision and Inertial Measurement Unit(IMU). This work aims at obtaining pure hough space and extract line segments with high confidence value from it finally. We divide this approach into two steps as follows:

Constructing primary probabilistic hough space: a primary probabilistic hough space is extracted from single frame which measures each line segment as probability value. In this section, an efficient Hough Transform with edge gradient constraints [16] is employed for line segments extraction and a CNN-based classifier is proposed for line segments classification. The proposed probabilistic hough space is constructed by the outputs of this classification networks and each point in this space describes the possibility of that the corresponding line segment is valid. Finally, we would use a threshold ξ(which is set to 0.7) to choose the final valid line segments from the probabilistic hough space.

Filtering probabilistic hough space across frames by IMU and vision data fusion: due to the disturbance of occlusion, vehicle pose and classification error, the primary probabilistic hough space extracted from single frame isn't reliable. For example(fig.7), when the pose of the vehicle changes, the classification results of the corresponding line segments become very different from before, that would make the same lane markings have different values in the probabilistic hough space. A Kalmen Filter is employed finally to smooth the probabilistic hough space across frame sequence. As the movement of vehicle, line segments extracted from images always have different position in hough space at different time, though they lie on the same lane markings. Movement information provided by the IMU makes it possible to align previous line segments in the same hough space which is significant for filtering. The final filtered probabilistic hough space is used to extract the final line segments. Line segments with low possibility will be eliminated and those with high values will be kept and tracked in the proposed probabilistic hough space.

Related works will be introduced in Section 2. In Section 3, we describe the construction of the primary probabilistic hough space depending on single frame. In Section 4, the primary probabilistic hough space is filtered across frames by the fusion of IMU and vision data. Finally, detailed experiments are discussed in this paper. Fig.1 shows the workflow of the proposed method.

2. Related Works

Lane detection play a fundamental role in current intelligent driving systems such as Advanced Driver Assistance System(ADAS) or autonomous driver system. A large amount of vision-based methods have been proposed.

2.1. Conventional algorithms without CNNs

In conventional lane detection approaches, edge is a common and important feature for extraction of lane structure. In [2],[3] and [4], Canny is used to extract and locate the edge position in image. However, there still exist a large amount of background noise in edge-map, and result would be worse when the scenario become more complicated such as rainy day. Lots of pre-processing algorithms are proposed to strengthen the feature of lane-markings. In [2], a LDA model is applied to make it more distinguishable between the lane-markings and background in RGB color space. A brightness stretching function named PLSF is proposed in [3] which makes lane-markings become more clearly than before. Each edge extraction method have its own strength and weakness, so [5] combines different strategies and use local threshold to extract edge, which make the edge extraction more robust. Prior information and Top-to-Bottom constraints are actually useful for eliminating false detection. For example, meaningful edge points are always located in the neighbor of line segments. Thus, in [4], a two-stage feature extraction method is proposed.

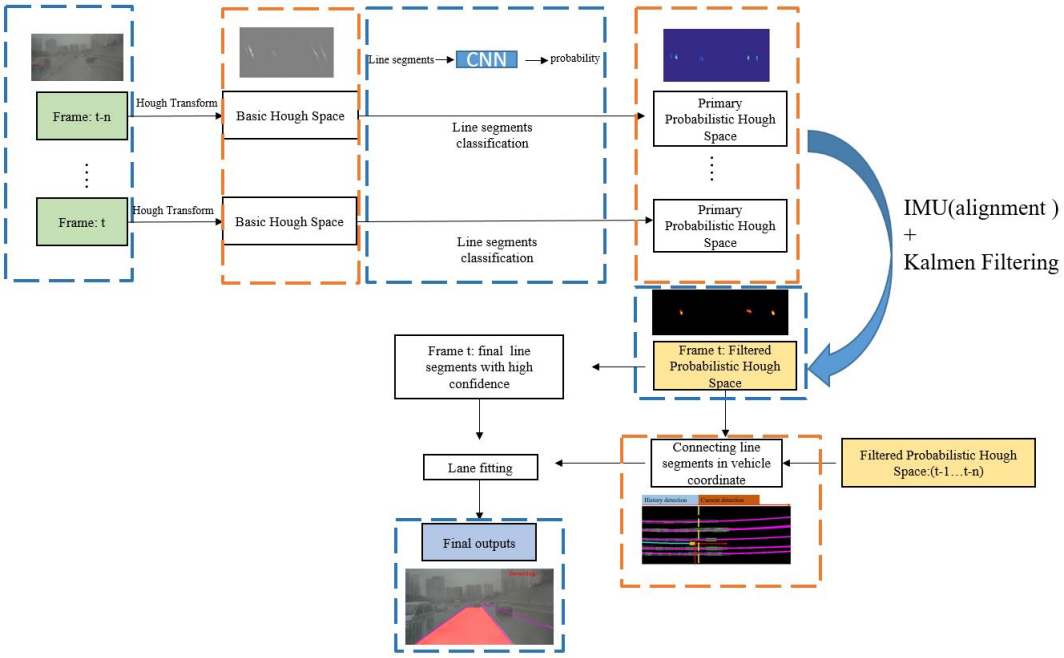

Figure 1. Workflow of the proposed approach: Hough Transform and Classification networks are used to extract the primary probabilistic hough space. Kalmen filtering is introduced to smooth the probabilistic hough space across frames, where sequential information is employed. Movement information provided by IMU is applied to make the previous line segemnts aligned in the current vehicle coordinate system.

Lane structure is a higher-level feature than edge. Hough Transform is a classical and robust approach to extract line segments from image. In order to purify these extracted line segments, constraints like parallelism are used, besides, [6] uses SVM to classify line segments. In [7] and [8], approaches to estimating the vanishing-point position are introduced and they use the road tendency information provided by vanishing-point to estimate the optimal parameters of the curve model. A Conditional Random Function (CRF) model is also proposed to extract lane structure in [9], where they extract many superpixels and use CRF to solve this multiple association task, finally, the best association among superpixels is solved to express the lane structures.

2.2. Lane detection with CNNs

Convolutional neural networks free us from designing handicraft features and rules, which have achieved state-of-art performance in many data sets. In [10], a multi-task network named VPG-net is proposed where multi-task training is proved that can improve the network performance. Fully convolutional networks for semantic segmentation are very suitable to solve lane detection problem, and its encoder-decoder structure have been used in many research such as work of[14,15]. However, post-process is necessary to cluster those fore-ground pixels into different lane instances after segmentation. Instance segmentation networks would be helpful to integrate semantic segmentation and this cluster post-process. In [11], an instance segmentation network is proposed, which can extract pixels on lanes and divide them into different lane instances. To improve the capacity of extracting spatial structure from image, [12] have designed a Spatial CNN (SCNN), which can make the best of the relationship between pixels across rows and columns in a layer. Generative adversarial networks(GANs) are also studied in this field, for example, EL-GAN [13] uses a Generative adversarial networks(GANs) and embedding loss to train an end-to-end network.

3. Single Frame: Primary Probabilistic Hough Space via Lane Markings Extraction

In this section, a primary probabilistic hough space is constructed by the line segments extraction and classification. Firstly, a combination of Hough Transform and RANSAC algorithm is employed to extract line segments efficiently. Then, the proposed CNNs networks is used to classify these line segments and construct the primary probabilistic hough space by using the output confidence for each line segment.

3.1. Line segments extraction by Hough Transform and RANSAC

An efficient Hough Transform [16]is used in this paper. Actually, traditional Hough Transform would bring much extra computation for its large voting range of direction which usually ranges from 0 to 360 degrees. Edge direction is employed to limit the voting range of direction. Defining the edge direction as ϕ and setting $H(\rho, \theta)$ as the Hough space, θ is limited by the right part of equation (1) in this paper.

$$\rho = c * \cos(\theta) + r * \sin(\theta) \quad \theta \in [\phi - \delta \ \phi + \delta] \tag{1}$$

This approach can make the extraction of line segments more efficient and reduce noise at the same time.

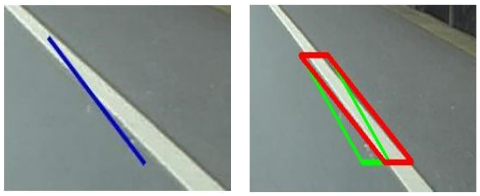

(a) (b)

Figure 2. (a) Example of line segment disturbed by edge noise. (b) Region-of-Interests are proposed by line segments (green: before revision. red: after revision).

However, these line segments extracted by Hough Transform is easily influenced by noisy edge-map just as the fig.2(a) shows. A revision process is carried out by RANSAC. These line segments provide RANSAC with numbers of Regions-of-Interest(ROI), and RANSAC is used to extract the best line segments in these regions. Detailed information is described by Algorithm 1. It's proved that this method is able to get better line segments (fig.2(b)).

Algorithm 1 : Revise line segments by RANSAC, R represents ROI and M is the edge-map, l is the final line segments

Input: R,M
Output: l
  function REVISEHT(R, M)
    while *iter* **do**
      $(P1, P2) \leftarrow Get\ edge\ points\ randomly\ from\ (R, M)$
      $\hat{l} : (\hat{k}, \hat{b}) \leftarrow Use\ (P1, P2)\ to\ fit\ straight\ line$
      if $\hat{l}$ *is better than* l **then** l=$\hat{l}$:$(\hat{k}, \hat{b})$
      end if
      $iter = iter - 1$
    end while
  end function

Preprints (www.preprints.org) | NOT PEER-REVIEWED | Posted: 15 April 2019 doi:10.20944/preprints201904.0175.v1

Peer-reviewed version available at Sensors 2019, 19, 2305; doi:10.3390/s19102305

Table 1. Structure of our classification network

Layer Index	1	2	3	4	5	6
Layer Name	Data	Conv+Relu	Pooling	Conv+Relu	Interp	Conv
Layer Index	7	8	9	10	11	12
Layer Name	Pooling	Conv	Pooling	Inner-Product	Inner-Product	Softmax

3.2. Constructing primary probabilistic hough space by classification networks

After line segments extraction, a post process is necessary to eliminate false line segments such as those lie on rails or trucks. In this paper, we propose a novel probabilistic hough space to measure each line segment by the metrics of possibility in hough space. Valid line segments which extracted from lane markings are labeled with high possibility in this proposed space(fig.6). A CNNs based classification networks is proposed to classify line segments and this probabilistic hough space is constructed by the outputs of the classification networks like fig.5 shows. We use a threshold ξ(which is set to 0.7) to choose the final valid line segments from the probabilistic hough space.

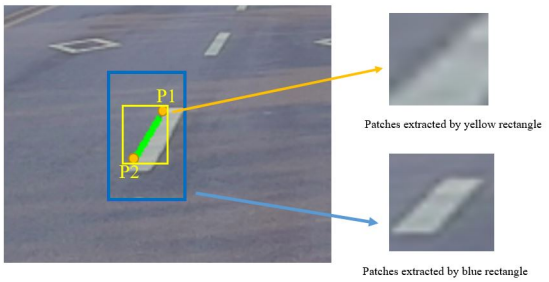

Figure 3. Yellow rectangle is proposed by the two endpoints (P1,P2) of line segments. Blue rectangle is proposed by two new calculated diagonal points by equation 3

(a) (b)

Figure 4. (a) Positive samples.(b) Negative samples.

Table 1 shows the structure of this network. Input image of this network is provided by each line segment. The diagonal points of these input images will be calculated according to each line segments. Fig.3 describes the process of extracting patches by using line segments.

Firstly, defining (x_1, y_1) and (x_2, y_2) are two endpoints of line segment l in vehicle coordinate, and k is the slope of l. W is the max width of traffic lane. Two new endpoints $(\hat{x}_1, \hat{y}_1)$ and $(\hat{x}_2, \hat{y}_2)$ could be obtained according to equation (3). Finally, these two new diagonal points can be projected into image plane by equation 2 and provide us with a reasonable patch like the blue one in fig.3.

$$s * \begin{pmatrix} c \\ r \\ 1 \end{pmatrix} = \boldsymbol{H} * \begin{pmatrix} x \\ y \\ z \\ 1 \end{pmatrix} \tag{2}$$

Preprints (www.preprints.org) | NOT PEER-REVIEWED | Posted: 15 April 2019 doi:10.20944/preprints201904.0175.v1

Peer-reviewed version available at Sensors 2019, 19, 2305; doi:10.3390/s19102305

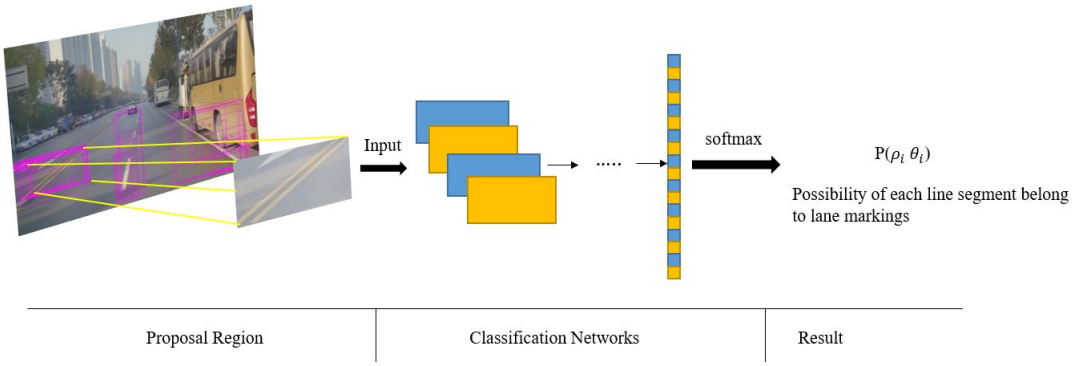

Figure 5. Process of line segments classification by using the proposed network: the inputs are proposed by line segments and this classification networks is used to choose valid line segments.

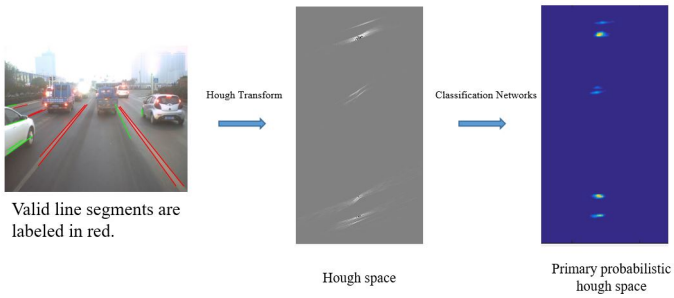

Figure 6. Primary probabilistic hough space.

$$
\begin{aligned}
(\widehat{x}_1, \widehat{y}_1) &= (x_1, y_1) + (-\frac{k}{|k|} \times w, -\frac{w}{|k|}) \\
(\widehat{x}_2, \widehat{y}_2) &= (x_2, y_2) + (\frac{k}{|k|} \times w, \frac{w}{|k|})
\end{aligned}
\tag{3}
$$

A training and testing dataset is established just as fig.4 shows. The positive samples are proposed by line segments which are belong to traffic lane markings and negative samples are proposed by false line segments. Total number of 50000 patches have been collected.

4. Sequential Frames: Filtered Probabilistic Hough Space via IMU and Vision Data

Obviously, lane markings won't appear and disappear suddenly in some position of road, if a line segment suddenly appear in the some place, but no lane markings exist here before, then this line segment is possibly a false one. On the contrary, if valid line segments usually appear in the some place, the possibility value of line segments there would keep high even the detection is disturbed by kinds of noises. However, the primary probabilistic hough space mentioned above is easily disturbed by the occlusion, movement of vehicle and classification error(fig.7). Thus, a Kalmen Filter is used to smooth the primary probabilistic hough space across sequence frames in this section. Movement information provided by IMU is applied to make the line segments extracted at different times aligned in the same hough space.

Preprints (www.preprints.org) | NOT PEER-REVIEWED | Posted: 15 April 2019 doi:10.20944/preprints201904.0175.v1

Peer-reviewed version available at Sensors 2019, 19, 2305; doi:10.3390/s19102305

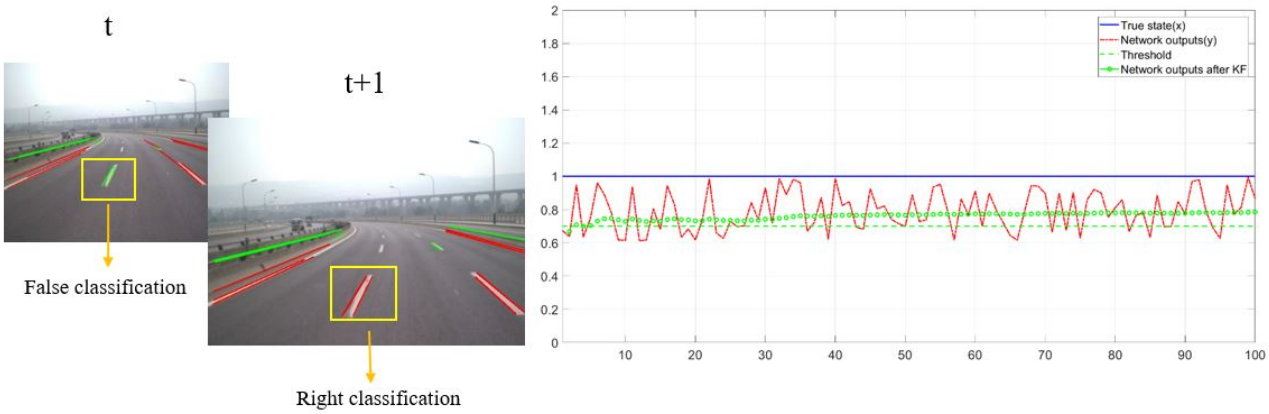

Figure 7. Left:due to the vehicle movement and the classification error of networks, the same line segment has different classification results at time *t* and *t+1*. Right: recording the outputs of networks for the same line segment at different time, and plotting the final prediction after kalmen filtering

4.1. Filtering primary hough space with Kalmen Filter

Setting x as the possibility value of a line segment l and y is the output confidence of the classification networks. Theoretically,x is equal to 1 if l is valid or else x is equal to 0. The state-transition matrix A is set to 1 and the noise matrix B is set to 0 because the attribute of the l should keep consistent with the previous frames. The observation matrix C is set to 1 and the observation noise D is caused by the vehicle movement and the classification error of networks. Equations 4 are the state equation for kalmen filtering.

$$\begin{aligned} x_t &= A * x_{t-1} + B \\ y_t &= C * x_t + D \end{aligned} \tag{4}$$

Line segment l has different position at different times in Hough Space because of the movement of vehicle, and it's necessary for kalmen filtering to obtain its observed value y from sets of probabilistic hough spaces which extracted at different times. So an alignment of $l_{t-1}(\rho_{t-1}, \theta_{t-1})$ and $l_t(\rho_t, \theta_t)$ should be solved in the Hough Space(Figure .9).

The filtered probabilistic hough space describes the probability from sequence consistency perspective about whether a line segments is belong to traffic lane markings or not and that is better and more robust than the primary probabilistic hough space. The result of this smooth process by using sequential information is showed by fig.7.

4.2. Align previous line segments in current Hough space

Firstly, projecting $l_{t-1}(\rho_{t-1}, \theta_{t-1})$ from previous vehicle coordinate into the current coordinate by using IMU information, which include velocity V=*(vx, vy, vz)*, acceleration A=*(ax, ay, az)* and Euler Angle (α, β, γ). Defining $([x^1_{t-1}, y^1_{t-1}, z^1_{t-1}], [x^2_{t-1}, y^2_{t-1}, z^2_{t-1}])$ as the position of l at time $t-1$ in vehicle coordinate, and its position at time t can be calculated by equation 7(i=*1,2*). Finally, (ρ_t, θ_t) is solved by perspective mapping 2 and equation 8.

Preprints (www.preprints.org) | NOT PEER-REVIEWED | Posted: 15 April 2019 doi:10.20944/preprints201904.0175.v1

Peer-reviewed version available at Sensors 2019, 19, 2305; doi:10.3390/s19102305

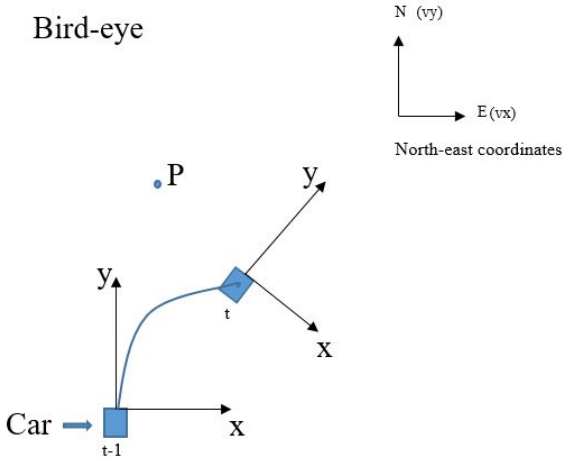

Figure 8. Calculating the position of object P in vehicle coordinate at different time. Velocity V and acceleration A are measured in North-east coordinates.

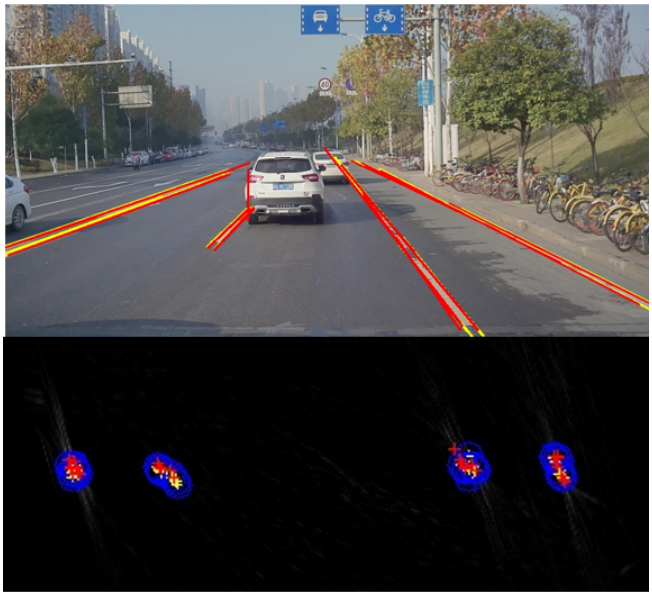

Figure 9. The result of alignment during neighbor frames. Current detection is labeled in Red and the previous is labeled in yellow.(Both in image plane and in Hough Space)

$$R(\alpha,\beta,\gamma) = \begin{pmatrix} 1 & 0 & 0 \\ 0 & \cos\alpha & \sin\alpha \\ 0 & -\sin\alpha & \cos\alpha \end{pmatrix} * \begin{pmatrix} \cos\beta & 0 & -\sin\beta \\ 0 & 1 & 0 \\ \sin\beta & 0 & \cos\beta \end{pmatrix} * \begin{pmatrix} \cos\gamma & \sin\gamma & 0 \\ -\sin\gamma & \cos\gamma & 0 \\ 0 & 0 & 1 \end{pmatrix} \tag{5}$$

$$\Delta T = \int_{t-1}^{t} V(t) + \frac{1}{2} \times A(t) \times t^2 dt \tag{6}$$

$$\begin{bmatrix} x_t^i \\ y_t^i \\ z_t^i \end{bmatrix} = R(\Delta\alpha, \Delta\beta, \Delta\gamma) * \begin{bmatrix} x_{t-1}^i \\ y_{t-1}^i \\ z_{t-1}^i \end{bmatrix} + R(\alpha_t, \beta_t, \gamma_t) * \Delta T \tag{7}$$

Preprints (www.preprints.org) | NOT PEER-REVIEWED | Posted: 15 April 2019 doi:10.20944/preprints201904.0175.v1

Peer-reviewed version available at Sensors 2019, 19, 2305; doi:10.3390/s19102305

$$\theta = \arctan(-\frac{r^1 - r^2}{c^1 - c^2}) + \frac{\pi}{2}$$
$$\rho = c * \cos(\theta) + r * \sin(\theta) \tag{8}$$

However, precision alignment is hard to achieve due to some factors such as the noise of IMU and the error of perspective mapping. So we regard all the $(\widehat{\theta}, \widehat{\rho})$ as projection of $l_{t-1}(\rho_{t-1}, \theta_{t-1})$

$$(\widehat{\theta} - \theta_t)^2 + (\widehat{\rho} - \rho_t)^2 <= r \tag{9}$$

4.3. Final lane fitting by using the result of sequential detection

By connecting valid line segments detected across frames like fig.10 shows, lane fitting could be solved with more sequential information. It plays a role similar to curvature tracking in many other works, but has more specific history information for decision. Equation (7) is employed to align previous results in current coordinate system, the final result is displayed by fig.10. These kind of lane-map will provide more global clues than single frame, which make the detection more stable.

In order to give the final outputs, a region-growth algorithm is used to divide these foreground points into different lane instances and a parabolic model is used to fit each lane in current vehicle coordinate. Fig.10 shows the whole process of this part. In order to limit the risk of over-fitting, L2 norm is added into our loss function displayed by equation (10). In equation (10), α_1 and α_2 are tradeoff coefficients.

$$E = \alpha_1 \sum (ax^2 + bx + c - y)^2 + \alpha_2 \|a\|^2 \tag{10}$$

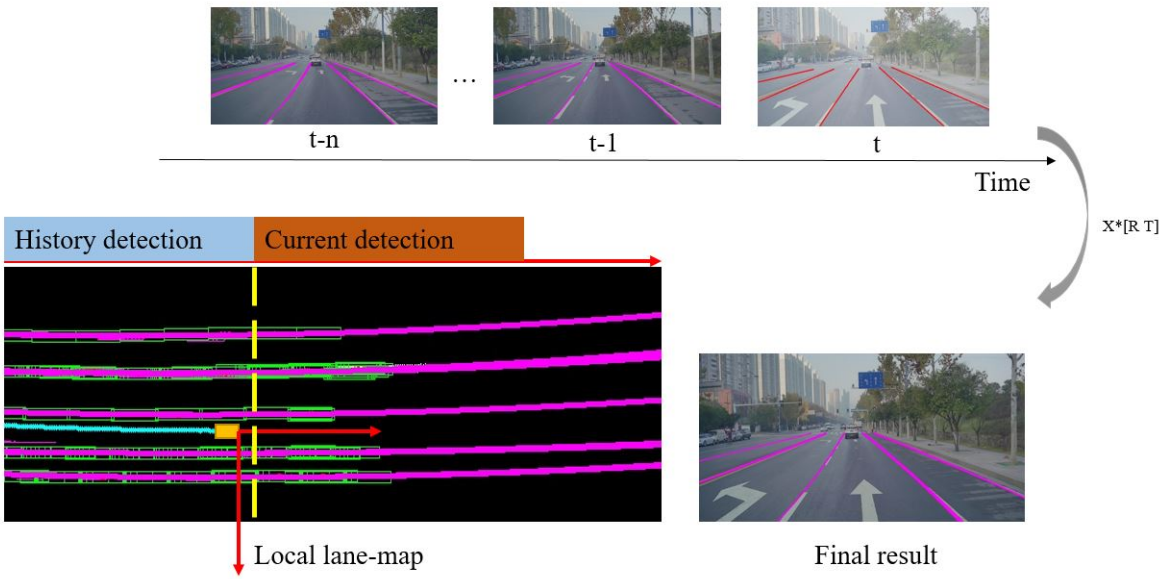

Figure 10. Local lane-map is constructed by connecting those recorded results from *t-n* to *t* in the same vehicle coordinate. It makes the final output more stable by providing useful information for the fitting stage in a larger spatial and time scale than single frame.

5. Experiments

In order to perform detailed experiments, we create our own dataset include images and IMU information using a AX7 vehicle(fig.12). Different road scenarios and weather conditions are contained such as Sunday and rainy day. Due to the need of training our classification networks, we create our own training and testing dataset like fig.4.

Peer-reviewed version available at Sensors 2019, 19, 2305; doi:10.3390/s19102305

To evaluate our algorithm, we choose four parts of road data to test the performance of our method, which contain rainy and sunlight conditions, and 667 pictures are annotated(fig.11). Those annotated pictures which size is [940, 1824] are labeled in the form of line segments like what fig.11 displays. Standard to decide whether a line segment is valid or not is showed by equation (11), where we define Er is the total offset between the detected line segments $\{(x_i, y_i)\}$ and the ground truth $\{(\hat{x}_i, \hat{y}_i)\}$ and n represents the length of the labeled line segments.

$$Er = \frac{1}{n}\sum_{i=1}^{n} |y_i - \hat{y}_i| + |x_i - \hat{x}_i| \quad (Er < T) \tag{11}$$

If Er is smaller than T, then we regard this detected line segment as valid detection. In this paper, T is set to 80.

Figure 11. Ground truth is labeled in the form of line segments

Figure 12. AX7 platform

This section is divided into two parts. In the first part, detailed analysis about the line segments extraction with classification will be introduced. Experiments about the work of the filtered probabilistic hough space will be discussed in the second part, where the fusion of IMU and vision is employed. Comparison experiment between the proposed method in [11] and our method is going to be introduced.

5.1. Performance of the classification networks

The performance of our classification networks is tested under Caltech dataset [22]. This dataset contains four video sequences which were all sampled from urban area. Easy conditions and challenging scenarios are all included such as shadows or writings. It's necessary to mention that we just detect 2-lanes in this part, in other words, we just detect lanes which are on the current lane. A comparison with other algorithms is discussed under this dataset, which use the metrics of Accuracy Rate(AR) and False Negative Rate(FNR).

Fig.13 shows the test result of the proposed method on Caltech dataset. The table 2 shows that the proposed method for line segments extraction and classification have a good performance compared

Peer-reviewed version available at Sensors 2019, 19, 2305; doi:10.3390/s19102305

to Aly's method and Niu's method. It's worth mentioning that our classification networks have a good generalization performance considering we didn't use caltech dataset to train our CNNs.

$$R = \frac{S}{N} \tag{12}$$

Figure 13. Performance on Caltech datasets

Table 2. Performance of each algorithm under caltech dataset

clip	total	Aly's method[18]		Niu's method[4]		Our method	
		AR(%)	FP(%)	AR(%)	FN(%)	AR(%)	FN(%)
cordova1	466	97.2	3.0	92.2	5.4	97.25	2.7
cordova2	472	96.2	38.4	97.7	1.8	97.05	1.2
washington1	639	96.7	4.7	96.9	2.5	95.84	3.7
washington2	452	95.1	2.2	98.5	1.7	95.63	3.1

5.2. Performance of the filtered probabilistic hough space

Lane detection is a kind of problem related to the sequence information very much. To make the best of history result, the proposed method integrates the information of IMU and vision where we use the Euler angle and velocity to align history result in a same coordinate. This alignment could help us match the same line segments at different times and obtain their confidence value, which make it possible to use sequential information for kalmen filtering and obtaining the filtered probabilistic hough space.

We use a threshold ξ(which is set to 0.7) to choose the final valid line segments from the filtered probabilistic hough space(equation).

$$Attribute = \begin{cases} valid, & p(\rho,\theta) \geq \xi \\ false, & p(\rho,\theta) < \xi. \end{cases} \tag{13}$$

A comparison between the performance of the primary probabilistic hough space and the filtered space by Kalmen Filtering is displayed by Fig. 14. It's easy to see the accuracy of line segments classification has been enhanced by using sequential information. We test the proposed method on four labeled datasets with the measurement metric of accuracy(ACC). Table 3 describes the accuracy of the classification when using primary probabilistic hough space and when using filtered probabilistic hough space by sequence frames. It's proved that the accuracy of line segments classification could be enhanced obviously after the filtering.

Table 3. Accuracy of the line segments extraction

Datasets	clip1	clip2	clip3	clip4
CNNs based classification	0.95	0.93	0.91	0.94
Filtered probabilistic hough space(sequential frames)	0.91	0.89	0.88	0.92

Peer-reviewed version available at Sensors 2019, 19, 2305; doi:10.3390/s19102305

Figure.14 shows the enhancement of classification accuracy by using the filtered probabilistic hough space. And figure .15 shows the final result of line segments detection and tracking. The first and third rows in figure.15 show the probabilistic hough space where the points with high brightness represent the possible valid line segments.

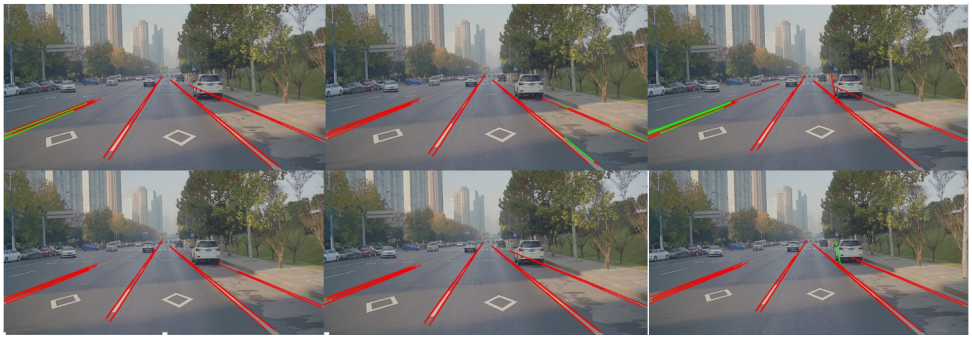

Figure 14. The first row shows the result depending on primary probabilistic hough space, and the second row shows the result extracted from the filtered probabilistic hough space. Valid line segments are labeled in red and false line segments are labeled in green.

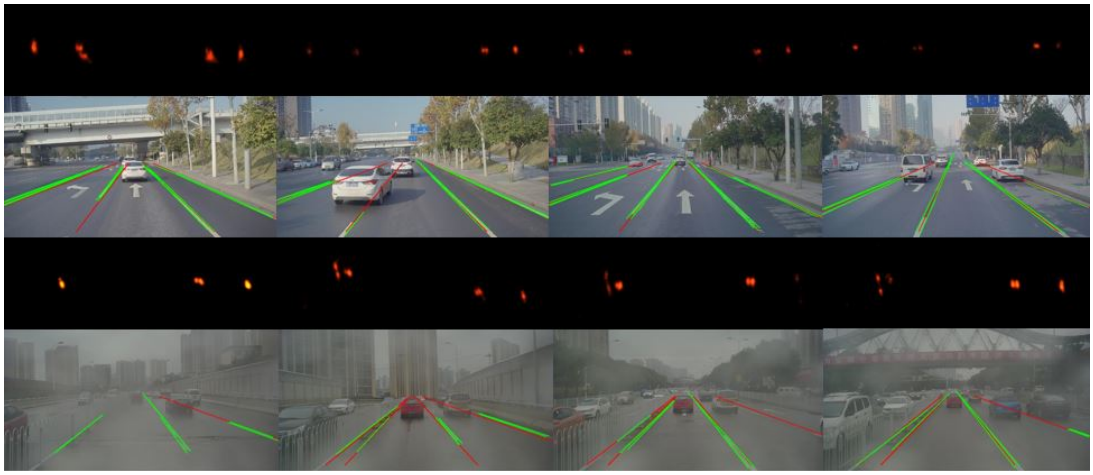

Figure 15. The first and third rows show the probabilistic hough space where the points with high brightness represent the possible valid line segments. The second and fourth rows show the result of line segments extraction where green line segments are the result of detection and red ones are the result of tracking.

The performance of the proposed approach in this paper is compared with Neven's method [11] by using the metrics described in equation.11. It can be seen from table 4 that the proposed method in this paper perform better than Neven's method sometimes, especially, we have a lower false positive rate than their method all the time due to the use of sequential information. However, both of Neven's method and our method perform not very well on the metrics of TPR, it's hard to detect those in the distance.

Table 4. Performance of each algorithm under our own dataset

clip	total	Neven's method[11]		Our method	
		TP(%)	FP(%)	TP(%)	FP(%)
part1	927	61.8	6.7	72.2	0.6
part2	174	78.2	38.5	72.9	1.5
part3	647	83.6	6.1	87.3	1.7
part4	713	82.5	5.9	76.5	0.1

By connecting information stored in lane-map, lane fitting could be solved with more sequential information. The result of final curve fitting is showed by fig.17. Figure.16 displays the result under kinds of scenarios.

Figure 16. Detection under different scenarios.

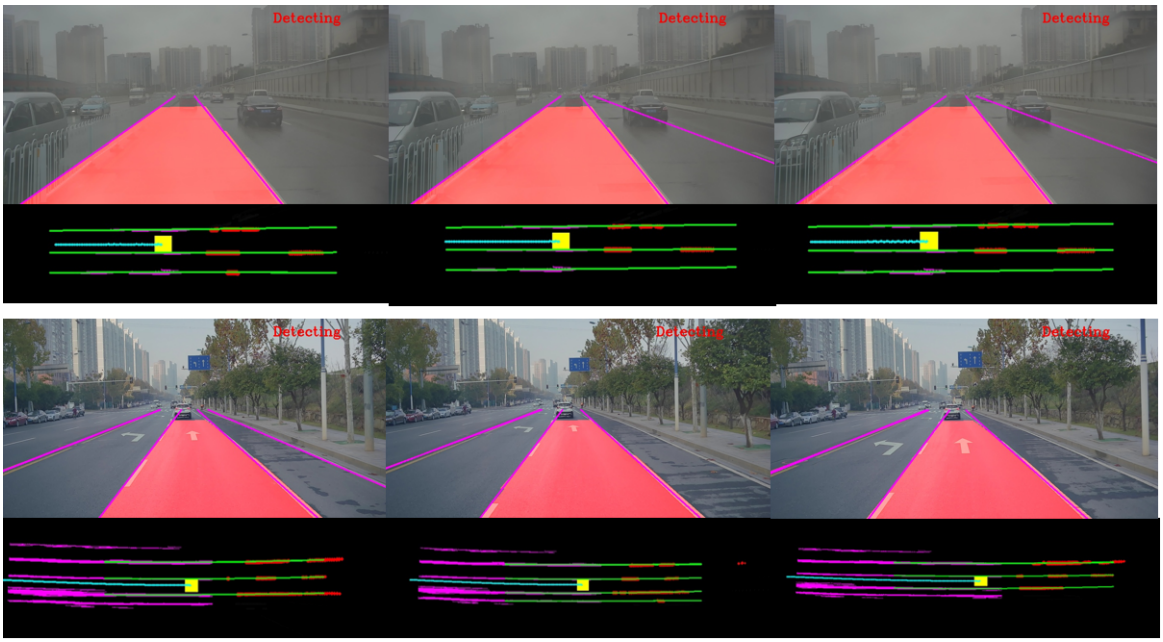

Figure 17. Result of final curve fitting based on lane-map.

6. Conclusion

In this paper, a multi-stage hough transform is proposed for our lane detection task by fusing the IMU and vision data. An efficient Hough Transform and a classification CNNs are introduced to extract and classify line segments from images. By using the outputs of the proposed classification networks, a novel primary probabilistic hough space could be constructed. In our work, we use a threshold ξ(which is set to 0.7) to choose the final valid line segments from the probabilistic hough space. However, the primary probabilistic hough space mentioned above is easily disturbed by the occlusion, movement of vehicle and classification error. Then, Kalmen filtering is used to smooth the probabilistic hough space across sequence frames. IMU is applied to make the previous line segments aligned in hough space. The filtered probabilistic hough space is finally used to eliminate false line segments with low possibility and output the line segments with high confidence. Our algorithm has few details need to be improved, for example, the proposed classification CNNs shall use more global

information to improve classification accuracy. More developments will be studied to improve the performance of our algorithm in the future work.

Acknowledgments

This work was supported by NSFC Grants 6147330.

References

1. Author1, T. The title of the cited article. *Journal Abbreviation* **2008**, *10*, 142–149.
2. Yoo H , Yang U , Sohn K . Gradient-Enhancing Conversion for Illumination-Robust Lane Detection[J]. IEEE Transactions on Intelligent Transportation Systems, 2013, 14(3):1083-1094.
3. Gaikwad V , Lokhande S . Lane Departure Identification for Advanced Driver Assistance[J]. IEEE Transactions on Intelligent Transportation Systems, 2014, 16(2):1-9.
4. Jianwei N , Jie L , Mingliang X , et al. Robust Lane Detection Using Two-stage Feature Extraction with Curve Fitting[J]. Pattern Recognition, 2016, 59(C):225-233.
5. Pollard E , Gruyer D , Tarel J P , et al. Lane Marking Extraction with Combination Strategy and Comparative Evaluation on Synthetic and Camera Images[J]. Conference Record - IEEE Conference on Intelligent Transportation Systems, 2011.
6. Zhao K , Meuter M , Nunn C , et al. A novel multi-lane detection and tracking system[C]// Intelligent Vehicles Symposium (IV), 2012 IEEE. IEEE, 2012.
7. Zhou S , Jiang Y , Xi J , et al. A novel lane detection based on geometrical model and Gabor filter[C]// Intelligent Vehicles Symposium. IEEE, 2010.
8. Ozgunalp U , Fan R , Ai X , et al. Multiple Lane Detection Algorithm Based on Novel Dense Vanishing Point Estimation[J]. IEEE Transactions on Intelligent Transportation Systems, 2016, 18(3):1-12.
9. Hur J , Kang S N , Seo S W . Multi-lane detection in urban driving environments using conditional random fields[C]// Intelligent Vehicles Symposium. IEEE, 2013.
10. Lee S , Kim J , Yoon J S , et al. VPGNet: Vanishing Point Guided Network for Lane and Road Marking Detection and Recognition[J]. 2017.
11. Neven D , De Brabandere B , Georgoulis S , et al. Towards End-to-End Lane Detection: an Instance Segmentation Approach[J]. 2018.
12. Pan X , Shi J , Luo P , et al. Spatial As Deep: Spatial CNN for Traffic Scene Understanding[J]. 2017.
13. Ghafoorian M , Nugteren C , Baka, N, et al.EL-GAN:Embedding Loss Driven Generative Adversarial Networks for Lane Detection[J]. 2018.
14. Wang, Ze and Ren, Weiqiang and Qiang, Qiu.LaneNet: Real-Time Lane Detection Networks for Autonomous Driving.2018.
15. Zhang W , Mahale T . End to End Video Segmentation for Driving : Lane Detection For Autonomous Car[J]. 2018.
16. Zhao Y , Pan H , Du C , et al. Principal direction-based Hough transform for line detection[J]. Optical Review, 2015, 22(2):224-231.
17. Author2, L. The title of the cited contribution. In *The Book Title*; Editor1, F., Editor2, A., Eds.; Publishing House: City, Country, 2007; pp. 32–58.
18. Aly M . Real time Detection of Lane Markers in Urban Streets[J]. 2014.
19. Behrendt K , Witt J . Deep learning lane marker segmentation from automatically generated labels[C]// 2017 IEEE/RSJ International Conference on Intelligent Robots and Systems (IROS). IEEE, 2017.
20. Bai D , Wang C , Zhang B , et al. Sequence Searching with CNN Features for Robust and Fast Visual Place Recognition[J]. Computers & Graphics, 2018, 70:270-280.
21. Xian Jiaotong University.TSD-Max.2017.http://trafficdata.xjtu.edu.cn/index.do
22. M,Aly.Caltech.2014.http://www.vision.caltech.edu/malaa/datasets/caltech-lanes/

Sample Availability: Samples of the compounds ..... are available from the authors.